secondary importance. (3) The effect of varying space velocity on pore-filling time is much less pronounced than either temperature or pressure, so long as the intrinsic rate remains relatively constant over the bed at the space velocities of interest. (4) The greatest effect on pore filling is caused by the assumed intrinsic carbon number distribution, i.e. the value of α (or α_1 and α_2 if this type of distribution occurs).

Some of the assumptions in the pore-filling model may limit the applicability of this analysis: (1) The assumption of a rate first order in H_2 and zero order in CO predicts an erroneously high rate of reaction on iron catalyst at very high conversion, where inhibition by water becomes significant. For other types of catalysts, different rate models may apply.

(2) With very fine pores, liquid will accumulate in pores more rapidly than predicted here, because of the effect of surface curvature on volatility. This is an especially important factor with catalysts containing zeolites. Under these conditions, deviations from the intrinsic product distribution on a Flory plot will occur at lower carbon numbers than suggested by the present analyses.

ACKNOWLEDGEMENT

This study was financially supported by the U.S. Department of Energy under grant No. DE-FG-81PC40771.

Table I. Reaction Conditions Assumed for Base Case Simulation.[a]

Variable	Value
Temperature	263°C
Pressure	790 kPa
Space Velocity	4000 cm^3 gas (S.T.P.)/h-g cat.
H_2/CO Feed Ratio	0.90
Pore Volume[b]	0.1 cm^3/g cat. (Anderson, 1956)
Flory Parameters: α_1	0.70
α_2	0.93
Z	0.95
Intrinsic Rate Constant	$k = 2.39 \times 10^8 \, e^{(-19700/RT)}$ μ moles H_2+CO converted/g cat.-min-kPa (Huff and Satterfield, 1984a). This gives values of 0.71, 1.3 and 2.2 at 232, 248, and 263°C, respectively.

[a]Fifty finite elements employed for computational purposes.

[b]While the pore volume is held constant at 0.1 cm^3/g cat. throughout this study, the pore-filling time is directly proportional to the value chosen.

Table II. Sensitivity of Predicted Time to Fill the First Pores with Liquid Product Anywhere in the Reactor Bed to Changes in the Reaction Conditions.[a]

Variable	Temperature (°C)	Pressure (kPa)	Rate Constant (μ moles)/g cat.-min-kPa	Space Velocity (cm³ gas/h-g cat.)	$(H_2/CO)_{in}$	% Total CO Conversion	Time (min.)
Pressure							
	263	1480	2.2	4000	0.90	64	129
	263	790	2.2	4000	0.90	35	311
	263	445	2.2	4000	0.90	20	709
Temperature							
	263	790	2.2	4000	0.90	35	311
	248	790	2.2	4000	0.90	21	517
	232	790	2.2	4000	0.90	12	925
Rate Constant							
	263	790	2.20	4000	0.90	35	311
	263	790	1.65	4000	0.90	27	441
	263	790	1.10	4000	0.90	18	725
	263	790	0.73	4000	0.90	12	1190
	263	790	0.44	4000	0.90	7.3	2330
	263	790	0.22	4000	0.90	3.6	5250
$(H_2/CO)_{in}$							
	263	790	2.2	4000	0.90	35	311
	263	790	2.2	4000	0.55	21	474
	263	790	2.2	4000	1.8	71	194
Space Velocity							
	263	790	2.2	10,000	0.90	14	375
	263	790	2.2	4000	0.90	35	311
	263	790	2.2	2000	0.90	68	275
	263	790	2.2	1500	0.90	86	272
	263	790	2.2	1000	0.90	100	275
	263	790	2.2	800	0.90	100	275
	263	790	2.2	600	0.90	100	276

[a]Unless otherwise noted, the base reaction conditions of Table I are assumed.

Table III. Comparison of Mathematical Methods for Pore-Filling Model with 10 elements. 263°C, 790 kPa, 800 cm^3 gas (S.T.P.)/g cat., $(H_2/CO)_{in}$ = 0.55.

Element Number	Volume in cm^3 of Condensed Product in Each Element at the Time of Pore Filling.[a]	
	Runge-Kutta Integration of Eq. 8	Simplified Method with Eq. 9
1 (inlet)	0.58	0.58
2	0.70	0.70
3	0.74	0.74
4	0.75[b]	0.75[c]
5	0.73	0.74
6	0.70	0.71
7	0.65	0.67
8	0.60	0.61
9	0.54	0.55
10 (outlet)	0.48	0.49

[a] A total of 75 g x 0.1 ml/g x 1/10g x 1/10 = 0.75 ml pore volume is available in each element.

[b] Element 4 is the first one predicted to fill after 480 min.

[c] Element 4 is the first one predicted to fill after 475 min.

NOMENCLATURE

A_m	Empirically determined constant representing the total rate of product accumulation as liquid in the catalyst pores of element m, mol/min
C_1, C_2, C_3	Constants independent of carbon number n
G_m	Total flow rate of vapor leaving element m, mol/min
j	Empirical coefficient for average organic product "C_jH_{2j}"
k	Intrinsic reaction rate constant of Fischer-Tropsch synthesis, μ mol/min-g cat.-kPa
m	Element number along the reactor bed; m = 1 at reactor inlet
m_n	Moles of carbon number n formed per total moles of organic product
MW	Average molecular weight of condensed product in catalyst pores, g/mol
n	Carbon number of organic product
n_c	Critical carbon number above which all products condense and below which all vaporize
P_{H_2}	Partial pressure of hydrogen, kPa
P_t	Reaction pressure, kPa
P_n^{vp}	Vapor pressure of carbon number, kPa
R	Ideal gas constant, 1.987 cal/K-mol
$-R_{H_2+CO}$	Intrinsic rate of carbon monoxide plus hydrogen consumption, mol/min-g cat.
$r_{n,m}$	Intrinsic rate of carbon number n produced in element m, mol/min.
t	Time, min.
T	Reaction temperature, K
X_m	Total moles of liquid in the catalyst pores of element m, mol
$x_{n,m}$	Carbon number n as liquid in the catalyst pores of element m, mol

$y_{n,m}$ Molar flow rate of carbon number n leaving element m as vapor, mol/min

$Y_{n,m}$ Moles of carbon number n in vapor effluent of element m per total moles of organic vapor

Z Mole fraction of product produced by the α_1 distribution

Greek Letters

α Probability of chain growth

β Dependence of vapor pressure on carbon number; $P_n^{vp} = C_1\beta^n$

LITERATURE CITED

Anderson, R.B. in Emmett, P.H., Ed., "Catalysis IV"; Reinhold: New York, 1956. (Chapter two)

Anderson, R.B.; Karn, F.S.; Shultz, J.F. Bull. U.S. Bur. Mines 1964, No. 614.

Dictor, R.A.; Bell, A.T. Ind. Eng. Chem. Process Des. Dev. 1983, 22, 678.

Dry, M.E. in Anderson, J.R.; Boudart, M., Eds., "Catalysis--Science and Technology 1"; Springer-Verlag: New York, 1981. (Chapter four)

Huff, G.A., Jr., Sc.D. Thesis, M.I.T., Cambridge, MA 1982.

Huff, G.A., Jr.; Satterfield, C.N. Ind. Eng. Chem. Process Des. Dev. 1984a, in press.

Huff, G.A., Jr.; Satterfield, C.N. J. Catal. 1984b, 85, 370.

Zwolinski, B.J.; Wilhoit, R.C. "Handbook of Vapor Pressures and Heats of Vaporization of Hydrocarbons and Related Compounds"; Thermodynamics Research Center: College Station, Texas, 1971.

APPENDIX A

Independence of Pore-Filling Rate on Time. As pointed out above, the rate of pore filling (eq. 9) in each finite element is assumed to be independent of time. For this simplification to be valid, the transition must be abrupt between those heavier products which condense as liquid in the pores and those lighter components which remain in the flowing vapor. Consider the extreme case in which some critical carbon number n_c exists above which all products condense and below which all vaporize. For n greater than n_c, eq. 6 becomes:

$$r_{n,m} = d(x_{n,m})/dt \tag{15}$$

Integration of eq. 15 with the initial condition that $x_{n,m} = 0$ at $t = 0$ yields:

$$x_{n,m} = r_{n,m}t \tag{16}$$

so that $A_m = \sum_{n>n_c}^{100} r_{n,m}$ from eq. 12. This implies that the total number of moles in the catalyst pores of element m should simply increase linearly with time, in accord with eq. 9.

The validity of this assumption (eq. 9) is borne out by two observations. First, the transition between products of carbon number n volatilizing and condensing typically occurs over a range of less than about 10 carbon numbers (e.g. see Figure 3). The transition is even more sharp when the relative amounts of products being formed are accounted for because the rate of product synthesis decreases logarithmically with carbon number per the Flory equation (eq. 5). Second, eq. 8 was numerically integrated with a Runge-Kutta method for a few cases without making the assumption of constant pore-filling rate with time. The excellent agreement between this mathematical analysis and the simplified method of eq. 9 is evident in the example of Table III. Since the Runge-Kutta method requires an unacceptably long computational time for the solution to be

stable, the simplified method is employed in this paper.

Quite interestingly, eq. 8, and 10 or 11 imply that the composition of carbon number n does not change while material is collecting in the pores, at least not until the pore completely fills. For example, the mole fraction $x_{n,m}/X_m$ of carbon number n in the first element (m = 1) is:

$$x_{n,m}/X_m = r_{n,1}(P^{nc}G_1/P_t + A_1) \qquad (17)$$

This behaviour results from the pores being initially empty and the rate of condensation for each product of carbon number n having the same linear dependency on time. The independence of composition on time is also observed with the Runge-Kutta method so it is not an artifact by assuming eq. 9. However, if the pores initially contained liquid composition different from that predicted by eq. 17, the equations derived in this paper based on eq. 9 are invalid (such as eq. 10 or 11). For instance, consider the case in which products are held up in the oil phase surrounding the catalyst of a Fischer-Tropsch slurry reactor. Quantitative interpretations proposed to account for product condensation in the liquid carrier indicate that the mole fraction of carbon number n in the liquid phase depends on time (Huff, 1982; Dictor and Bell, 1983). This behaviour is explained by the total number of moles in the liquid remaining relatively constant, unlike pore condensation in a fixed-bed reactor, because of the overwhelming amount of liquid carrier present initially.

APPENDIX B

Dependence of Observed α at Higher Carbon Numbers. As discussed above, the apparent α based on the product vapor at higher carbon numbers is less than the true value. A mathematical relationship can be derived to account for this behaviour by examining the dependency of pore-filling on carbon number n.

Figure 17 is a plot of log P_n^{vp} versus n. Since the plot is linear, then:

$$P_n^{vp} = C_1 \beta^n \tag{18}$$

where β is the slope of the curve and C_1 is a constant independent of n. Values of β vary from 0.69 to 0.74 over the temperature range of interest (232 to 263°C). Consider only the heavy compounds such that eq. 16 applies and where the product distribution is represented by α_2 of eq. 5. It can be shown for $n > n_c$ that:

$$\frac{x_{n,m}}{x_m} = C_2(1-\alpha_2)\alpha_2^{n-1} \tag{19}$$

where C_2 is a constant at each element m, e.g., see Figure 2. Even though the moles of product in the vapor are negligibly small compared to that in the liquid, the amount volatilized is calculated by Raoult's law (eq. 7):

$$y_{n,m} = \frac{P_n^{vp} G_m x_{n,m}}{x_m P_t} \tag{20}$$

Substituting eq. (18) and (19) yields:

$$y_{n,m} = \frac{C_1 \beta^n G_m C_2 (1-\alpha_2)\alpha_2^{n-1}}{P_t} \tag{21}$$

or

$$y_{n,m} = C_3(\beta\alpha_2)^n \tag{22}$$

where C_3 is a constant at each element m and independent of n. Since $y_{n,m}$ is proportional to the mole fraction of C_n in total organic vapor, $Y_{n,m}$, then:

$$Y_{n,m} \propto \underbrace{(\beta\alpha_{2,actual})}_{\alpha_{observed}}{}^n \tag{23}$$

List of Figure Captions

Figure 1 — Predicted Volume Percent of Catalyst Pores Filled with Liquid Product and Predicted Average Molecular Weight Accumulated Liquid versus Bed Depth at Moment the First Pore is Completely Filled. Base Reaction Conditions of Table I.

Figure 2 — Predicted Carbon Number Distribution of Product Condensed as Liquid in the Catalyst Pores, at Moment of First Filling. Base Reaction Conditions of Table I.

Figure 3 — Predicted Distribution of Products Between the Vapor and Liquid Phases at the Moment the First Pore is Completely Filled. Base Reaction Conditions of Table I.

Figure 4 — Predicted Vapor Product Distribution at the Moment the First Pore is Completely Filled. Base Reaction Conditions of Table I.

Figure 5 — Predicted Volume Percent of Catalyst Pores Filled with Liquid Product versus Bed Depth at Moment the First Pore is Completely Filled. Base Reaction Conditions of Table I but with Total Pressure Varied.

Figure 6 — Predicted Average Molecular Weight of Accumulated Liquid Product versus Bed Depth. Base Conditions of Table I but with Total Pressure Varied.

Figure 7 — Predicted Volume Percent of Catalyst Pores Filled with Liquid Product versus Bed Depth at Moment the First Pore is completely Filled. Base Reaction Conditions of Table I but with Temperature Varied.

Figure 8 Predicted Average Molecular Weight of Accumulatec Liquid Product versus Bed Depth. Base Conditions of Table I but with Temperature Varied.

Figure 9 Predicted Volume Percent of Catalyst Pores Filled with Liquid Product versus Bed Depth at Moment First Pore is Filled. Base Reaction Conditions of Table I but with Space Velocity Varied.

Figure 10 Predicted Carbon Monoxide Conversion versus Bed Depth for Conditions in Figure 9.

Figure 11 Predicted Average Molecular Weight of Accumulated Liquid Product versus Bed Depth for Conditions in Figure 9.

Figure 12 Predicted Volume Percent of Catalyst Pores Filled with Liquid Product versus Bed Depth at Moment First Pore is Filled. Base Reaction Conditions of Table I but with a Single α Value Which is Varied.

Figure 13 Predicted Average Molecular Weight of Accumulated Liquid Product versus Bed Depth for Conditions in Figure 12.

Figure 14 Predicted Time to Fill the First Pore with Liquid Product, Anywhere in the Reactor. Base Reaction Conditions of Table I but with a Single α Value Which is Varied.

Figure 15 Predicted Time to Fill First Pore with Liquid Product Anywhere in the Reactor as a function of α. Base Conditions of Table I but for Selected Combinations of Temperature and Pressure.

Figure 16 Predicted Vapor Product Distribution in Reactor Effluent at Moment that First Pore is completely filled. Base case conditions of Table I, except that $\alpha = 0.85$.

Figure 17 Vapor Pressure of Paraffin of Carbon Number $\underline{n}$ versus n.

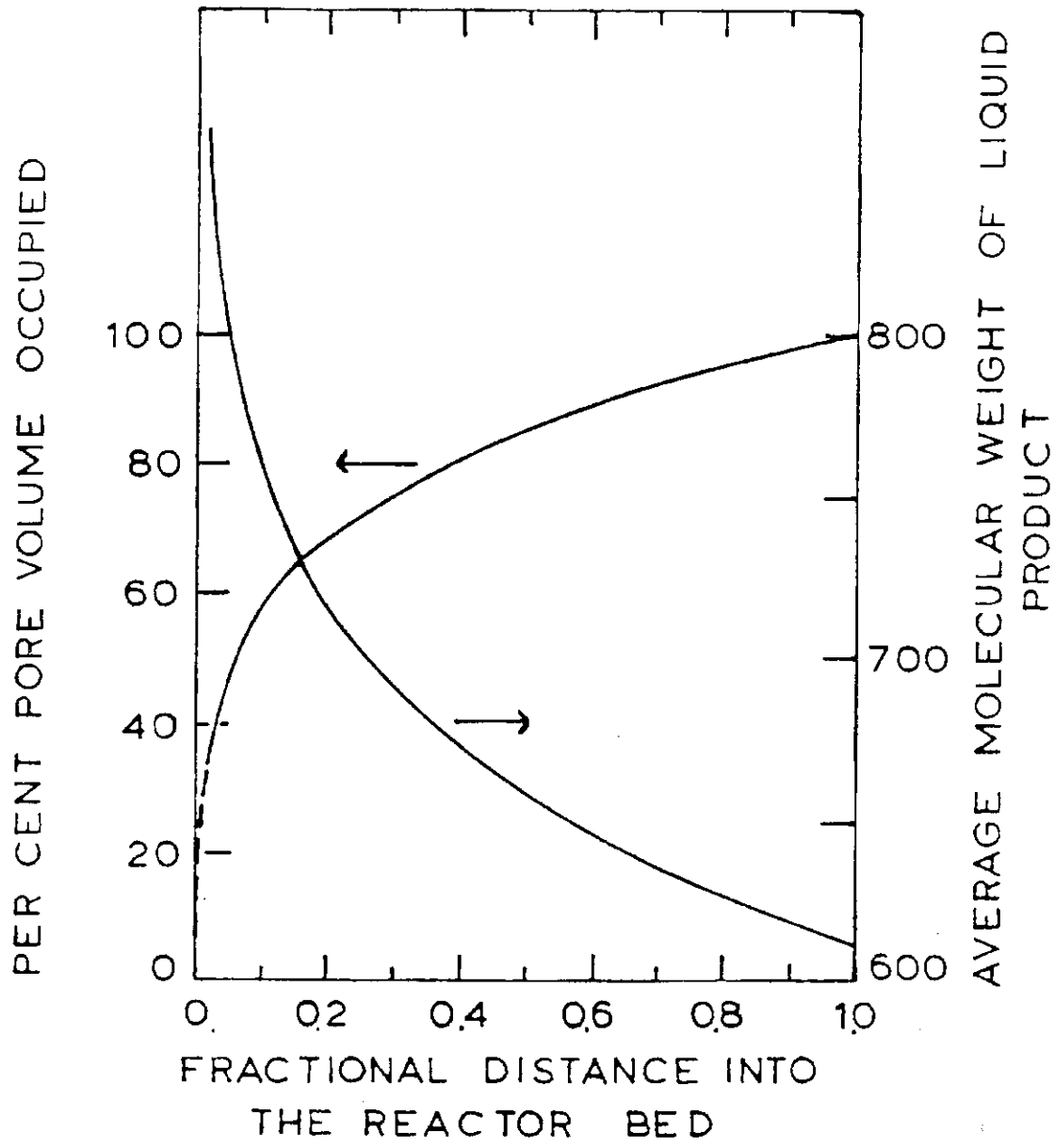
PER CENT PORE VOLUME OCCUPIED
100
80
60
40
20
0
800
700
600
AVERAGE MOLECULAR WEIGHT OF LIQUID PRODUCT
0
0.2
0.4
0.6
0.8
1.0
FRACTIONAL DISTANCE INTO THE REACTOR BED

FIGURE 1

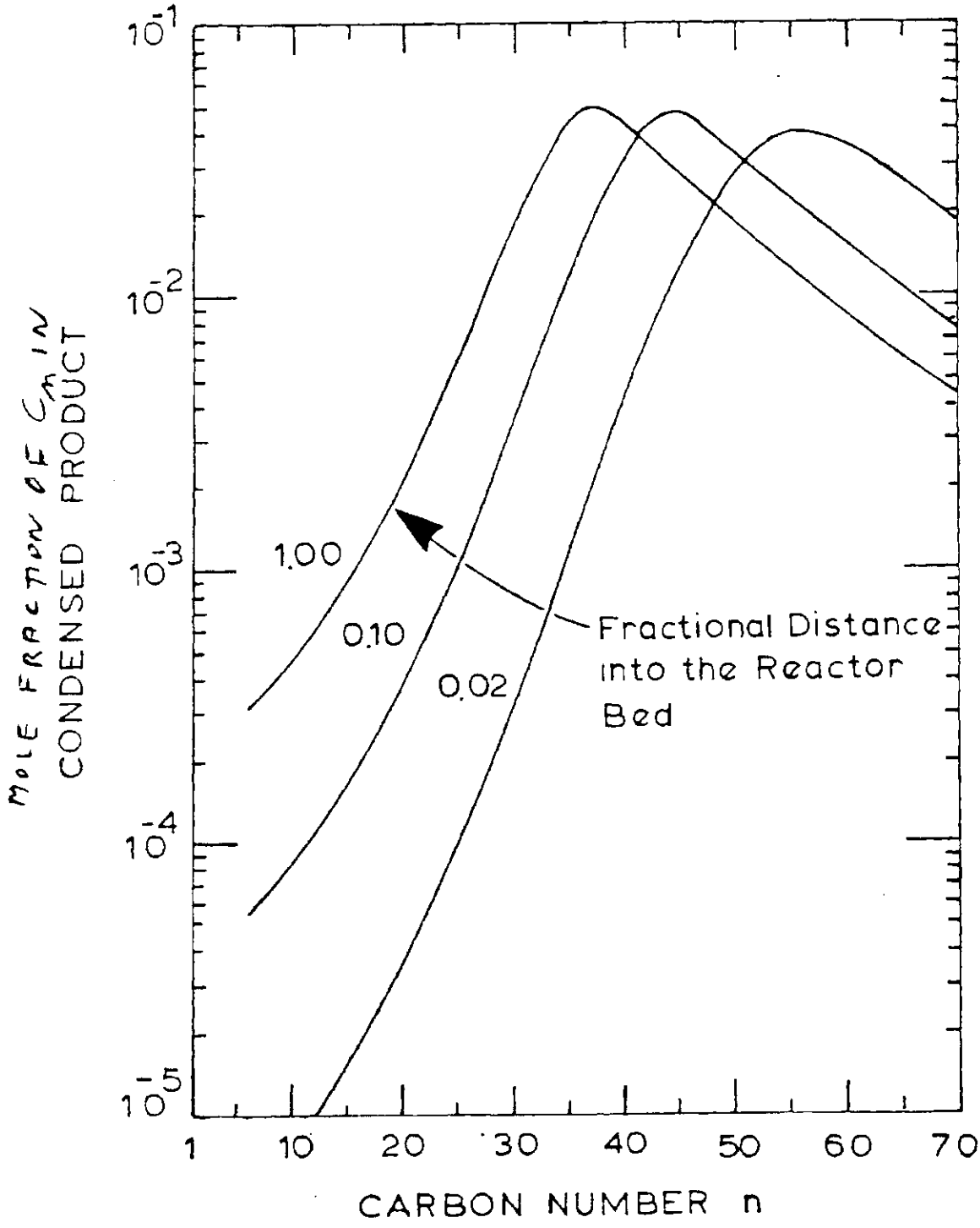
MOLE FRACTION OF C_n IN CONDENSED PRODUCT
10^{-1}
10^{-2}
10^{-3}
10^{-4}
10^{-5}
1.00
0.10
0.02
Fractional Distance into the Reactor Bed
1
10
20
30
40
50
60
70
CARBON NUMBER n

FIGURE 2

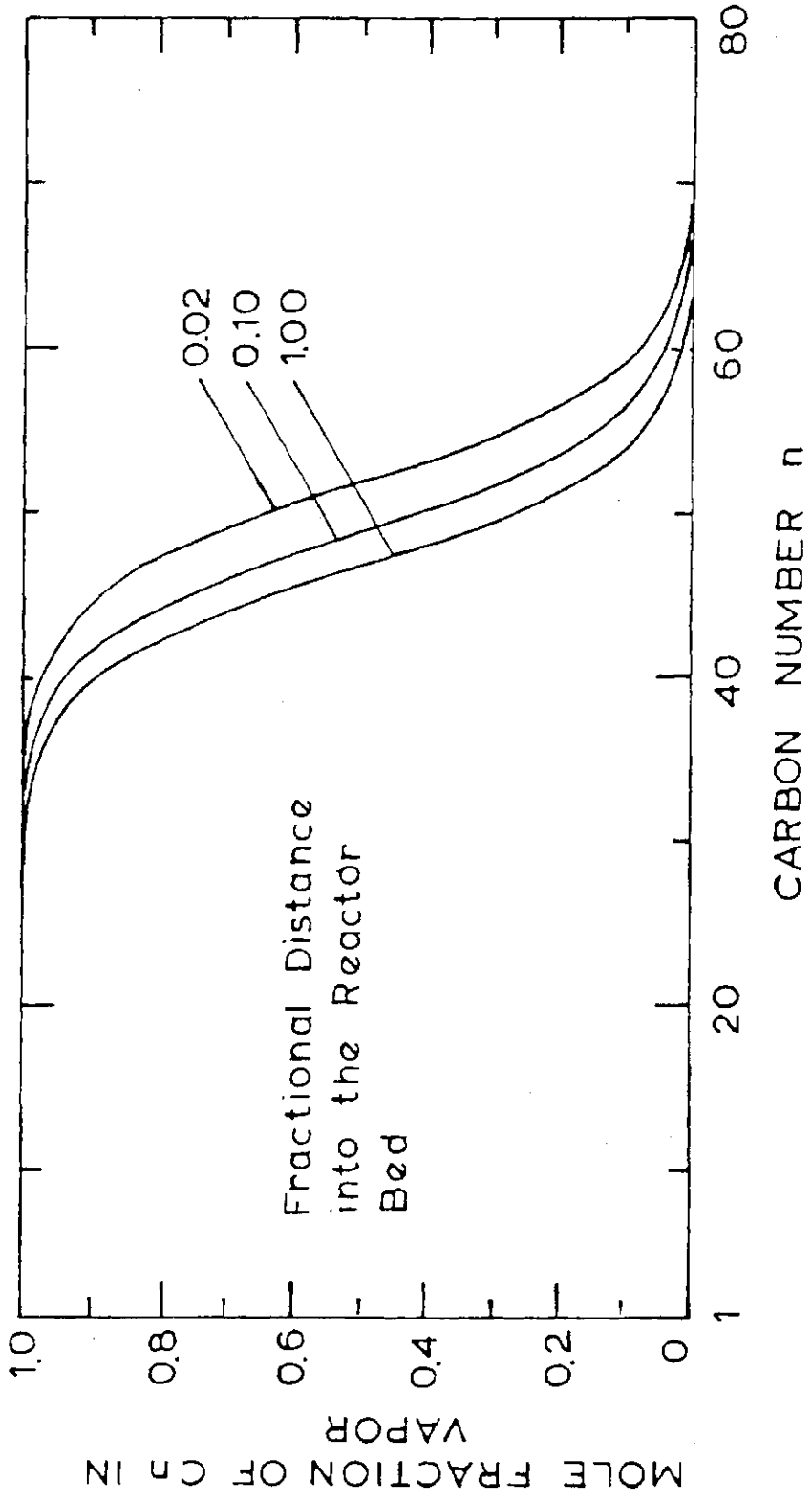
MOLE FRACTION OF Cn IN VAPOR
1.0
0.8
0.6
0.4
0.2
0
1
20
40
60
80
CARBON NUMBER n
0.02
0.10
1.00
Fractional Distance into the Reactor Bed

FIGURE 3

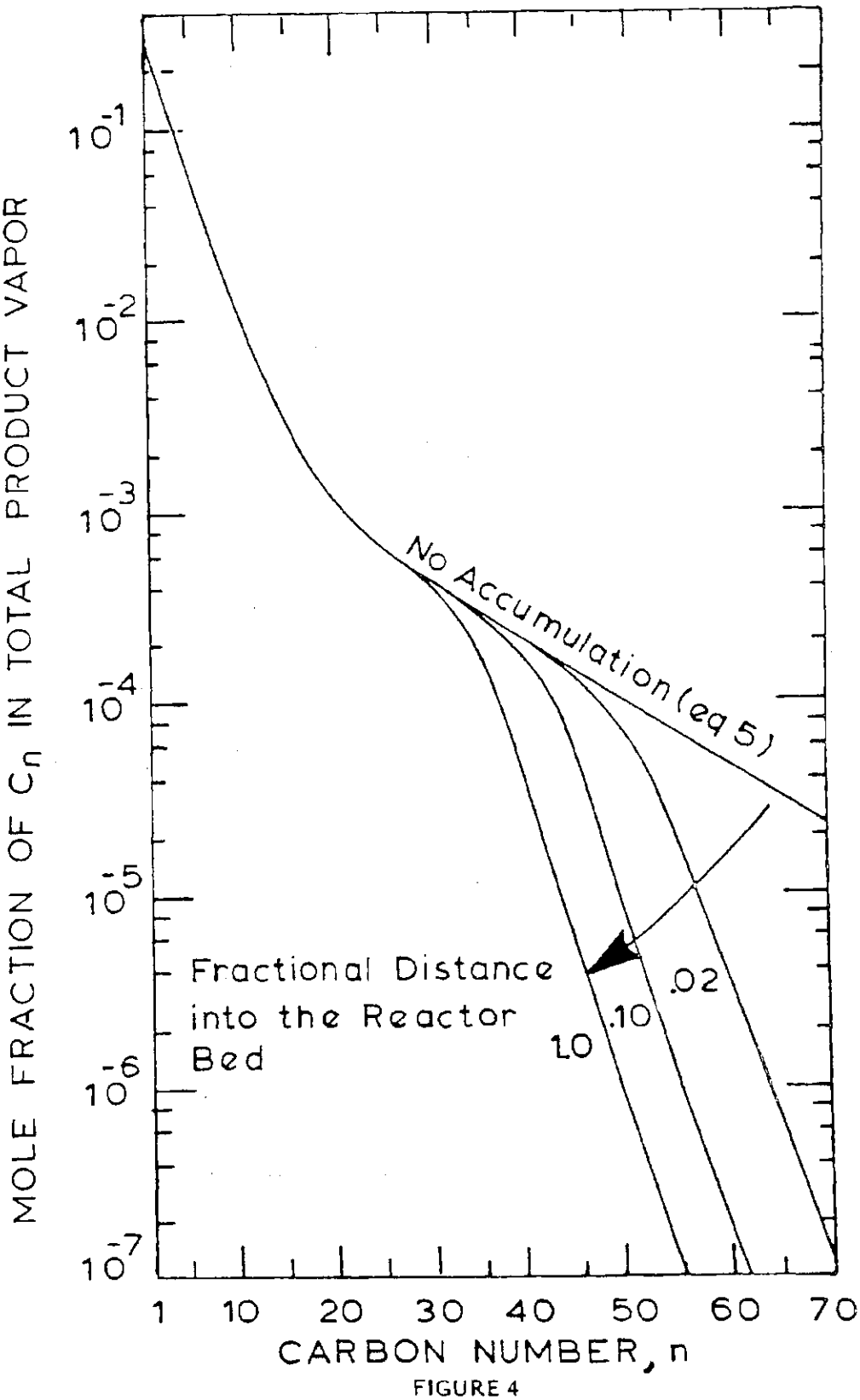
MOLE FRACTION OF C_n IN TOTAL PRODUCT VAPOR
10^{-1}
10^{-2}
10^{-3}
10^{-4}
10^{-5}
10^{-6}
10^{-7}
No Accumulation (eq 5)
Fractional Distance into the Reactor Bed
1.0
.10
.02
1
10
20
30
40
50
60
70
CARBON NUMBER, n

FIGURE 4

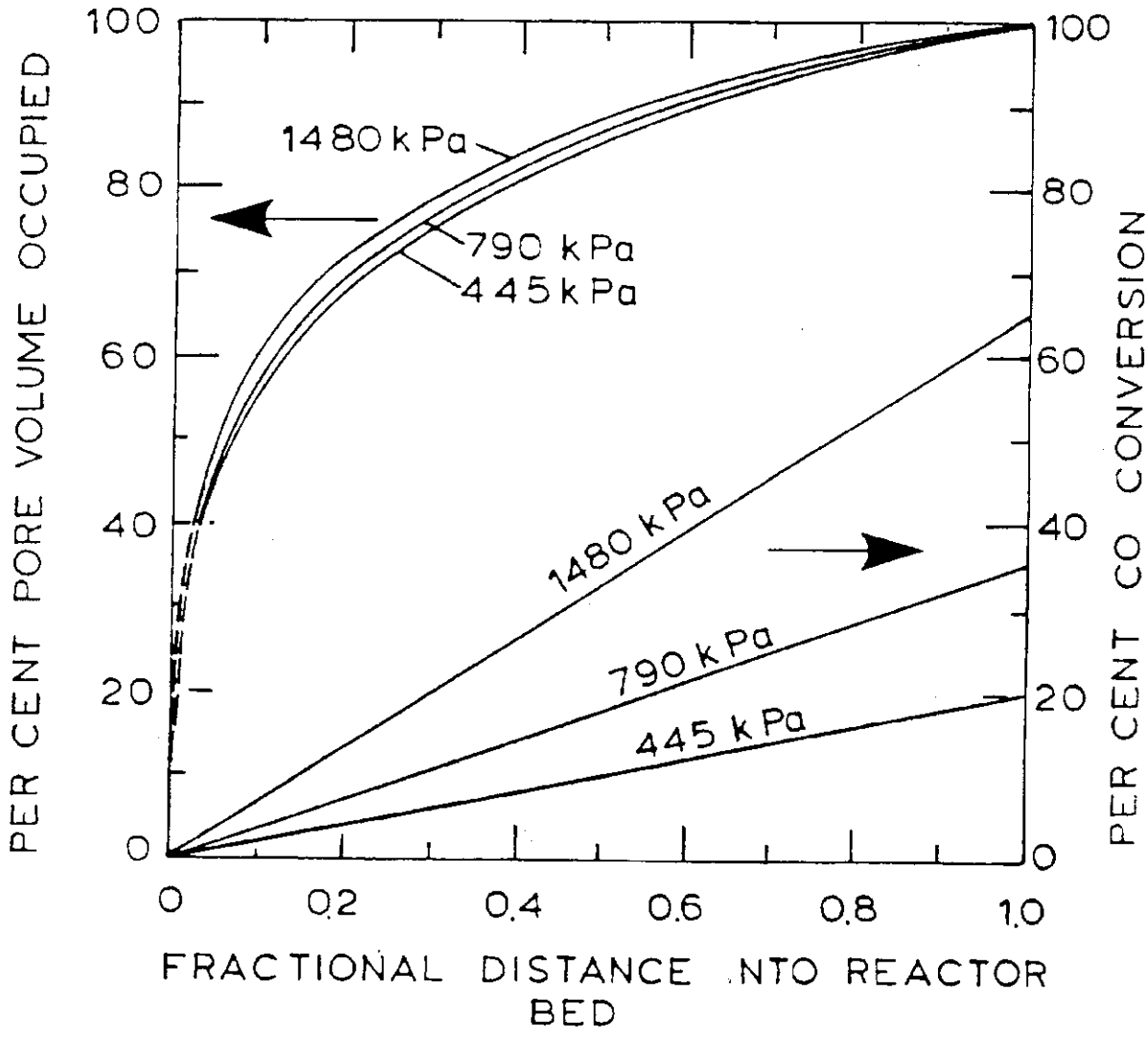
PER CENT PORE VOLUME OCCUPIED
PER CENT CO CONVERSION
100
80
60
40
20
0
1480 kPa
790 kPa
445 kPa
1480 kPa
790 kPa
445 kPa
0
0.2
0.4
0.6
0.8
1.0
FRACTIONAL DISTANCE INTO REACTOR BED

FIGURE 5

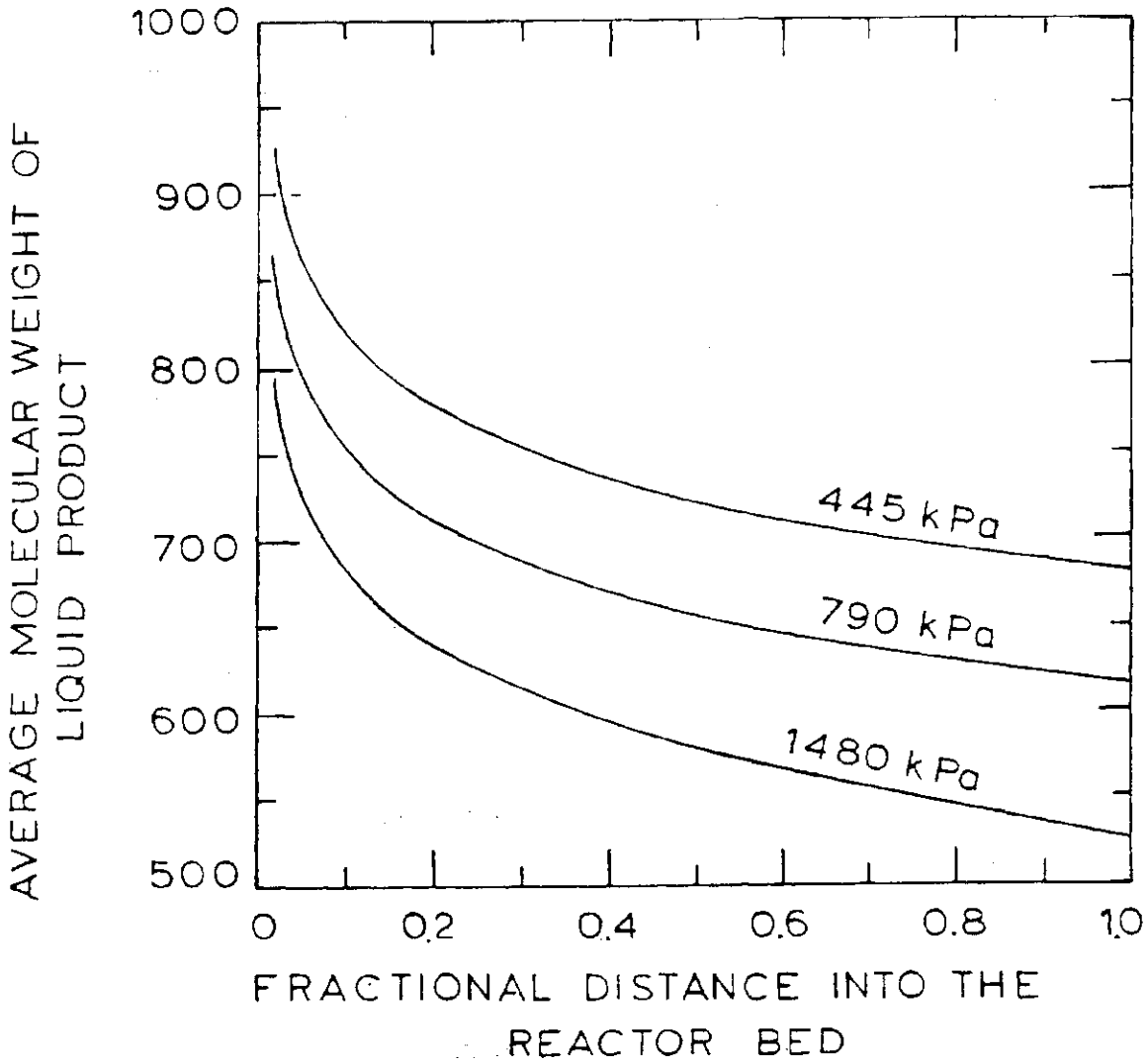
AVERAGE MOLECULAR WEIGHT OF LIQUID PRODUCT
1000
900
800
700
600
500
445 kPa
790 kPa
1480 kPa
0
0.2
0.4
0.6
0.8
1.0
FRACTIONAL DISTANCE INTO THE REACTOR BED

FIGURE 6

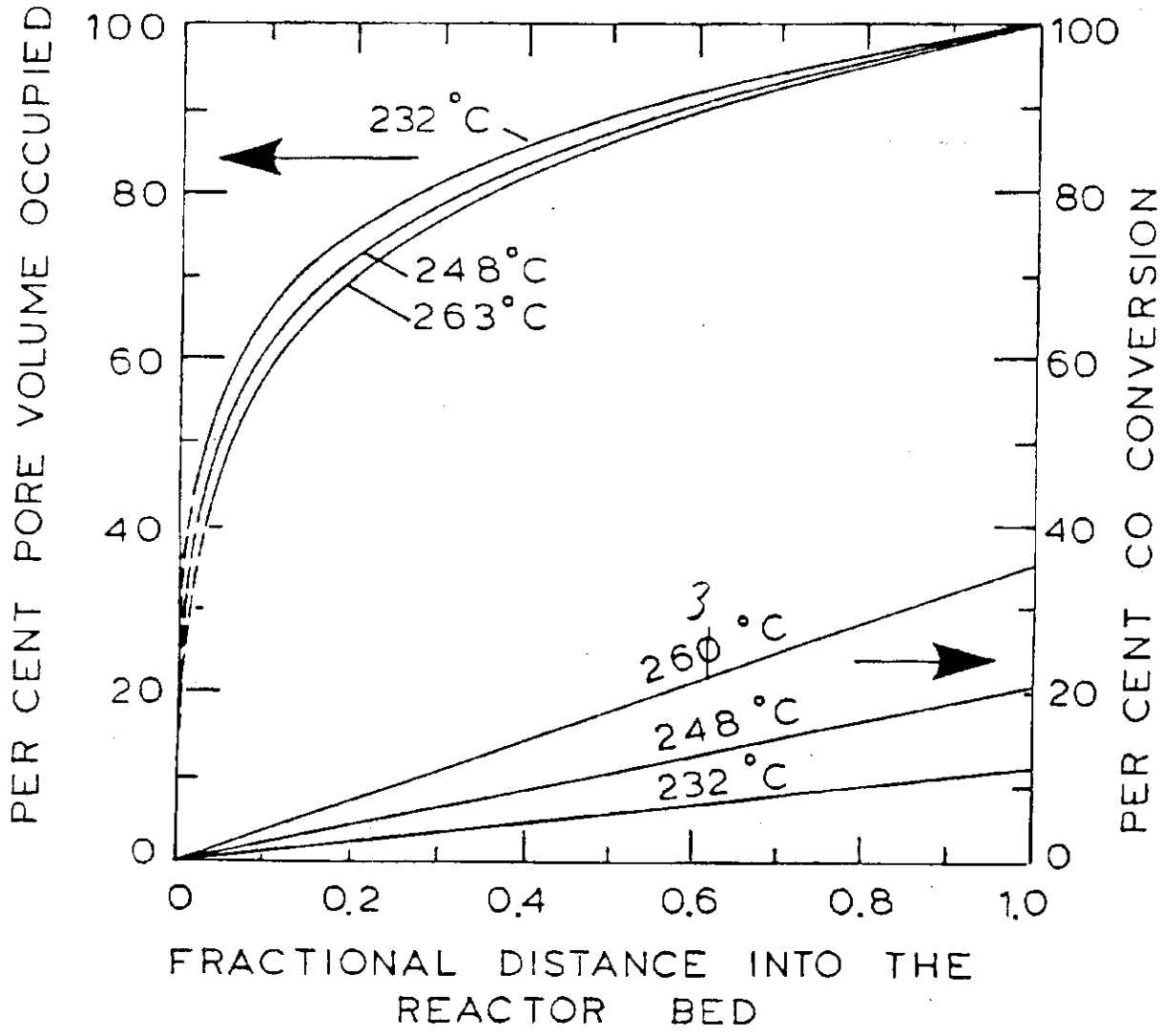
PER CENT PORE VOLUME OCCUPIED
PER CENT CO CONVERSION
100
80
60
40
20
0
232 °C
248 °C
263 °C
260 °C
248 °C
232 °C
0
0.2
0.4
0.6
0.8
1.0
FRACTIONAL DISTANCE INTO THE REACTOR BED

FIGURE 7

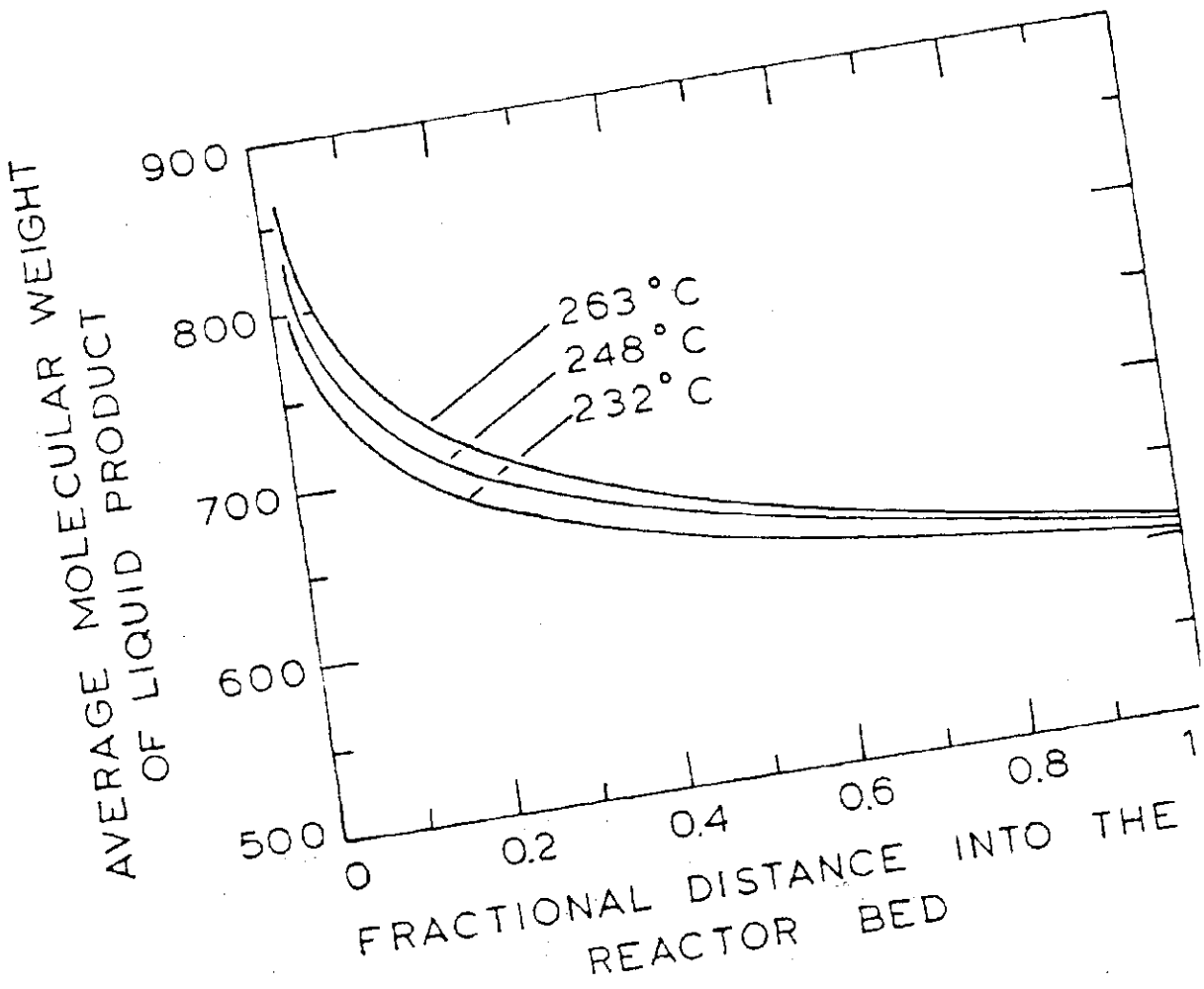
AVERAGE MOLECULAR WEIGHT OF LIQUID PRODUCT
900
800
700
600
500
263°C
248°C
232°C
0
0.2
0.4
0.6
0.8
1
FRACTIONAL DISTANCE INTO THE REACTOR BED

FIGURE 8